XVI CONGRESSO BRASILEIRO DE ENGENHARIA MECÂNICA
16th BRAZILIAN CONGRESS OF MECHANICAL ENGINEERING

SEMI-ANALYTICAL DETERMINATION OF HALO ORBITS VIA THE LINDSTEDT-POINCARÉ METHOD

Cristian Beauge
Universidade Nacional de Córdoba
Laprida 854, (5000), Córdoba, Argentina
E-mail: BEAUGE@DEM.INPE.BR

Gislaine de Felipe
Instituto Nacional de Pesquisas Espaciais - INPE
São José dos Campos - SP - 12227-010 - Brasil
Phone (123)256197 - Fax (123)25-6226
E-mail: GISLAINE@DEM.INPE.BR

Antonio Fernando Bertachini de Almeida Prado
Instituto Nacional de Pesquisas Espaciais - INPE
São José dos Campos - SP - 12227-010 - Brasil
Phone (123)256197 - Fax (123)25-6226
E-mail: PRADO@DEM.INPE.BR

Abstract. *This paper presents results of the application of the Lindstedt-Poincaré method for the determination of three-dimensional periodic orbits in the vicinity of the collinear Lagrange points in the restricted circular three-body problem. These solutions, known in the literature as "Halo" orbits, are of great practical importance and have been used as reference trajectories for several artificial satellites and probes launched in the last 20 years. The principal aim of this communication is to introduce a simple and straightforward analytical method for the computation of small-to-moderate amplitude solutions, together with an innovative approach for extending this approach to any amplitude, no matter how large. Examples of Halo orbits are shown in the case of the Earth-Moon system, and the results compared with numerical integrations of the exact differential equations.*

Key Words: Astrodynamics, Halo Orbits, Orbit Determination.

1. Introduction

Consider the circular restricted three-body problem in a rotating barycentric coordinate system *(X,Y,Z)*, such that both massive bodies (i.e. $m_1 > m_2 > 0$) are always located in the *X* axis, and the *XY* plane coincides with their plane of motion. In this scenario we find five equilibrium solutions, the so-called Lagrange points, which are denoted by L_i ($i=1,...,5$). Two of them (L_4 and L_5) are located in the *XY* plane forming equilateral triangles with the primaries. The remaining points all lie along the *X* axis: L_1 between both massive bodies, L_2 beyond and L_3 between m_1 and minus infinity. For values of m_2/m_1 smaller than a critical value, the equilateral points are stable. All three "collinear" points, on the other hand, are unstable for all values of the masses. They are usually referred to as fixed points of type *Center* x *Saddle* x *Center*; unstable (i.e. *Center* x *Saddle*) for motions in the plane, and stable (i.e. *Center*) in the *Z* axis. Three-dimensional periodic orbits around these unstable points, also unstable by nature, are called *Halo orbits*.

It seems at first hand that such trajectories are among the least desirable places in which to place an artificial satellite. Nevertheless, since the beginning of the 1970s serious studies began to be undertaken on this regard. Possibly the first was due to Farquhar. When NASA was still planning possible scenarios for the exploration of the Moon, serious consideration began to be placed on the problem of communication between the Earth and a hypothetical exploratory base located in the far side of the Moon. It is known that, due to the spin-orbit resonance between the Moon's rotational motion and its translation around the center of mass, the far side is always invisible from our planet, thus making impossible any contact with ground control. This question was analyzed, among others, by Farquhar (1970), Farquhar and Kamel (1973) and Richardson and Kary (1975). As a solution, they proposed the localization of a communication satellite in a Halo orbit around the L_2 Lagrange solution. Due to its periodicity and particular shape, the trajectory would avoid all periodic occultations by the Moon, assuring permanent contact with the astronauts. The question of the intrinsic instability of the orbit was solved proposing periodic station keeping maneuvers whenever the true trajectory departed sufficiently from the nominal solution.

Although the end of the *Apollo* project appeared as a serious blow to these projects, soon other applications of halo orbits were proposed and made reality. Examples are the satellites developed for the study of Solar wind in the vicinity of our planet. Solar wind consists of atoms and ions that are driven by the Sun. Studying their composition, astronomers hope to obtain important data to estimate the chemical composition of the Solar System at the time of its formation and, thus, are of great importance for models of planetary formation. However, there exist serious difficulties in the detection and analysis of Solar wind. Since it is made up of electrically charged particles, it is

deflected by the terrestrial magnetosphere and, consequently, cannot be studied from the vicinity of our planet. The only solution is to place a satellite outside the "bow shock".

Of all the possible orbits for such a satellite, the best suited is precisely a Halo orbit around the L_1 point of the Sun-Earth system. The main advantage over normal heliocentric orbits is the fact that it is always between the Sun and our planet, thus allowing a permanent observation of both bodies without eclipses of any sort. This type of orbit was used in 1978 by the probe ISEE-3 (*International Sun-Earth Explorer-3*), where it remained for several years. Almost twenty years later, the Solar wind in the L_1 point was once again monitored by the SOHO (*Solar & Heliospheric Observatory*), launched in 1995 and, more recently, by the ACE (*Advanced Composition Explorer*) launched in 1997, and still in operation. Probably the most ambitious projects are yet to come. The GENESIS probe (scheduled for 2002) will not only continue the observation of the Sun but will also collect samples of Solar wind and, after a three-year mission, bring them back to Earth. Thus it represents the first program, since Apollo, to bring extraterrestrial material to Earth.

In the present paper we review the determination of Halo orbits in the circular restricted three-body problem via a classical analytical method known as Lindstedt's Device or the Lindstedt-Poincaré method. Its main advantage over other analytical approaches lies in its simplicity and high precision. An important drawback, however, is the fact that it is only convergent for low to moderate amplitudes of the periodic orbits. We will therefore briefly introduce a modification of the equations of motion that allows us to overcome this limitation. The manuscript is organized as follows: Section 2 presents the equations of motion in the vicinity of a Lagrange fixed point, together with Richardson's expansion of the pseudo-potential terms. These equations form the basis for the application of the analytical method. Lindstedt's device is reviewed in Section 3, and explicit formula for Halo orbits are presented as well. Section 4 discusses the extension of the method for large-amplitude orbits. Section 5 shows examples of Halo orbits in the Earth-Moon and Sun-Earth systems, while comparisons with exact numerical simulations follow in Section 6. Finally, conclusions close the paper in Section 7.

2. Orbits in the Vicinity of the Collinear Lagrange Points

Since we are basically interested in orbits in the vicinity of one of the collinear equilibrium points, let us begin by introducing a transformation of coordinates (X,Y,Z)→ (x,y,z) to new variables centered around L_i:

$$\begin{aligned} X &= -\gamma_i x + \mu + A \\ Y &= -\gamma_i y \\ Z &= \gamma_i z, \end{aligned} \tag{1}$$

where γ_i is the distance from L_i to the nearest primary, and $A = -1 + \gamma_1$ (for L_1), $A = -1 - \gamma_2$ (for L_2). In terms of these new variables, the equations of motion can be written as (see Szebehely, 1967):

$$\begin{aligned} \ddot{x} - 2\dot{y} &= x - \frac{(1-\mu)}{r_1^3}(x-\mu) - \frac{\mu}{r_2^3}(x+1-\mu) \\ \ddot{y} + 2\dot{x} &= y - \frac{(1-\mu)}{r_1^3} y - \frac{\mu}{r_2^3} y \\ \ddot{z} &= -\frac{(1-\mu)}{r_1^3} z - \frac{\mu}{r_2^3} z \end{aligned} \tag{2}$$

Here $\mu = m_2/(m_1+m_2)$, $r_1^2 = (x-\mu)^2 + y^2 + z^2$ and $r_2^2 = (x+1-\mu)^2 + y^2 + z^2$. In order to develop the nonlinear terms in the right-hand side, we expand them as function of Legendre polynomials P_n, defined by means of the expression:

$$\frac{1}{\sqrt{(x-a)^2 + (y-b)^2 + (z-c)^2}} = \frac{1}{D} \sum_{n=0}^{\infty} \left(\frac{\rho}{D}\right)^n P_n\left(\frac{ax+by+cz}{D\rho}\right) \tag{3}$$

with $D^2 = a^2 + b^2 + c^2$ and $\rho^2 = x^2 + y^2 + z^2$. After some straightforward calculations (see Richardson, 1980) the equations of motion for the massless particle can be written in power series of the coordinates as:

$$\begin{aligned}
\ddot{x} - 2\dot{y} - (1+2c_2)x &= \sum_{n\geq 2}(n+1)c_{n+1}T_n \\
\ddot{y} + 2\dot{x} + (c_2 - 1)y &= y\sum_{n\geq 2} c_{n+1}R_{n-1} \\
\ddot{z} + c_2 z &= z\sum_{n\geq 2} c_{n+1}R_{n-1}
\end{aligned} \tag{4}$$

The c_n coefficients are given by:

$$c_n(\mu) = \frac{1}{\gamma_i^3}\left((\pm 1)^n \mu + (-1)^n \frac{(1-\mu)\gamma_i^{n+1}}{(1 \mp \gamma_i)^{n+1}}\right) \tag{5}$$

where the upper sign is used for L_1 and the lower for L_2. Functions T_n, R_n can be obtained by the following recurrence relations:

$$R_n(x,y,z) = -\frac{2n+2}{n+2}T_n + \frac{2n+3}{n+2}xR_{n-1} - \frac{2n+1}{n+2}\rho^2 R_{n-2} \tag{6.1}$$

$$T_n(x,y,z) = \frac{2n-1}{n}xT_{n-1} - \frac{n-1}{n}\rho^2 T_{n-2} \tag{6.2}$$

with initial values $T_0 = 1$, $T_1 = x$ and $R_0 = 1$; $R_1 = -3x$.

Equations (4) constitute our final expression for the motion of a massless particle in the vicinity of the collinear libration point L_i. Note that the right-hand side contains only nonlinear terms and that the expansion (3) in Legendre polynomials is convergent only for values of $\rho < 1$; this then constitutes a limit for the possible values of the amplitudes of the Halo orbits determined via this approach.

3. The Lindstedt-Poincaré Method

Amongst the various perturbation techniques applied to the problem of halo orbits, probably the simplest and most straightforward is the Lindstedt's device. Contrary to other approaches, it does not require extensive knowledge of the Hamiltonian perturbation methods or the development/use of complex algebraic computer software. Although the sheer size of the formulas may seem uncomfortable at first, they are very easily understood and, once the basis of the method is grasped, can be reproduced and extended with very little trouble. The basic idea of the method is as follows: Starting from the linearized system (i.e. zeroing all the right-hand members of Eq. (4)), we can determine the linear solution as:

$$\begin{aligned}
x &= \alpha e^{i\omega_0 t} \\
y &= \kappa\alpha e^{i\omega_0 t} \\
z &= \beta e^{i\nu_0 t}
\end{aligned} \tag{7}$$

where ω_0, ν_0 are the linear planar and off-plane frequencies of motion and α, β are the amplitudes (in complex notation) in the *x* and *z* axis respectively. Finally, κ is a constant that relates the amplitude in the *y*-axis with that in the other planar dimension. Now, we know that the inclusion of nonlinear terms (i.e. right-hand side of (4)) will yield a solution that will contain contributions from both the linear planar motion as well as the linear motion in the *z* axis. Thus, we can write the general solution as a Fourier series of the type:

$$\begin{pmatrix} x \\ y \\ z \end{pmatrix} = \sum_{i,j,k,l} \begin{pmatrix} X_{i,j,k,l} \\ Y_{i,j,k,l} \\ Z_{i,j,k,l} \end{pmatrix} \alpha^i \beta^j e^{\sqrt{-1}(k\omega + l\nu)t} \tag{8}$$

in terms of new complex coefficients $X_{i,j,k,l}$, $Y_{i,j,k,l}$, $Z_{i,j,k,l}$. We suppose similar expansions for the coefficients T_n, R_n in the right-hand sides. The values of the coefficients of Eq. (8) are obtained introducing these series into the original differential equations, identifying terms of equal harmonic and degree (in α and β) and solving the resulting algebraic equations. The new frequencies (also affected by the nonlinear terms) can be obtained as power series of the linear amplitudes α, β in the form:

$$\omega = \sum_{i,j} \omega_{i,j} \alpha^i \beta^j \tag{9.1}$$

$$\nu = \sum_{i,j} \nu_{i,j} \alpha^i \beta^j \tag{9.2}$$

where $\omega_{0,0} = \omega_0, \nu_{0,0} = \nu_0$.

The general quasi-periodic solutions, in which $\omega \neq \nu$, are usually referred to as *Lissajous* orbits and are of limited practical importance since they periodically cross the line of sight between both primaries. *Halo* orbits can be considered as a particular case of Lissajous trajectories, in the case of $\omega = \nu$. Unfortunately, periodic orbits, although present in the nonlinear system, have no linear counterpart. Thus, in order to use the Lindstedt-Poincaré method, we must reformulate our original system Eq. (4). This can be accomplished introducing a new function Δ (which will ultimately be set to zero) and rewriting the differential equations as:

$$\begin{aligned} \ddot{x} - 2\dot{y} - (1+2c_2)x &= \sum_{n\geq 2} (n+1) c_{n+1} T_n \\ \ddot{y} + 2\dot{x} + (c_2 - 1)y &= y \sum_{n\geq 2} c_{n+1} R_{n-1} \\ \ddot{z} + (c_2 - \Delta)z &= z \sum_{n\geq 2} c_{n+1} R_{n-1} \end{aligned} \tag{10}$$

Once again, this function can be expanded in power series of the amplitudes: $\Delta = \sum_{i,j} \Delta_{i,j} \alpha^i \beta^j$. The linear terms $\Delta_{1,0}$, $\Delta_{0,1}$ are now chosen so as to generate a periodic orbit in the linear system. The high-order terms $\Delta_{i,j}$ are finally chosen so as to guarantee $\Delta = 0$ (see Gomez *et al.* 1998, Andreu and Simo 1999, Gomez *et al.* 2000).

4. Extension to Large-Amplitude Orbits

The formula deduced in the previous section is convergent for all Halo orbits with amplitudes smaller than a certain critical value associated with $\rho = 1$ (see equation 3). This limit is not critical for most practical applications since the trajectories of most Halo-type artificial satellites do not extend beyond $\rho = 0.8$. Nevertheless, in some cases it proves important to (at least) analyze the structure of Halo orbits beyond this limit. In such a scenario, the formula deduced from Richardson' s expansion proves useless, and a different methodology must be employed. In this section we introduce such an approach. Although it implies a certain complication in the formula (and thus is not recommended for $\rho < 1$) it is convergent for all values of the amplitude.

We begin with equations (2). However, instead of expanding the right-hand sides in Legendre polynomials, we introduce two additional variables to our system:

$$\begin{aligned} s_1 &= \frac{(1-\mu)}{r_1^3} \\ s_2 &= \frac{\mu}{r_2^3} \end{aligned} \tag{11}$$

Differentiating these expressions, we can rewrite our new (extended) system as:

$$\begin{aligned} \ddot{x} - 2\dot{y} &= x - s_1(x-\mu) - s_2(x+1-\mu) \\ \ddot{y} + 2\dot{x} &= y - s_1 y - s_2 y \\ \ddot{z} &= -s_1 z - s_2 z \\ \dot{s}_1 &= -3 s_1 \frac{\dot{r}_1}{r_1} \\ \dot{s}_2 &= -3 s_2 \frac{\dot{r}_2}{r_2} \end{aligned} \tag{12}$$

The procedure to solve this system is similar to the one detailed in Section 3. We use the Lindstedt-Poincaré method in exactly the same manner. The difference with Richardson' s technique, however, lies in the expansion of the right-hand side of the last two equations. Instead of using Legendre polynomials, we work with operations on Fourier series. First, we use Eq. (8) to obtain a Fourier series of r_1, r_2. Since these quantities are always greater than zero, we can invert these series and obtain expressions for the coefficients of the series $(r_1)^{-1}$, $(r_2)^{-1}$. This can be done

analytically with little trouble, although a certain care must be taken with the manipulation of the coefficients. Introducing these into Eq. (12), we finally obtain formula analogous to those used in classical studies.

5. Results

This method was implemented and applied to both the Earth-Moon and the Sun-Earth sub-systems. In each we generated several Halo orbits around the Lagrangian point L_1 for different values of the linear amplitude β. Figure 1 shows the three-dimensional view and the x-y, y-z and x-z projections for the Earth-Moon case. Figure 2 shows the same views in the Sun-Earth system. The values used for β varied from 0.1 to 0.9 in steps of 0.1. Values of β higher than 0.9 gives very poor results and are not shown here. Figure 3 shows the variation of the non-linear frequency ω as a function of β. We can see that the period of the Halo orbit is very sensitive with respect to this amplitude; its value being significantly higher for the Earth-Moon system than for the Sun-Earth case. Figure 4 shows the variation of the amplitude in the x-direction α as a function of β. It is visible that the relation is close to linear for both systems and that the amplitudes are higher for the Sun-Earth system.

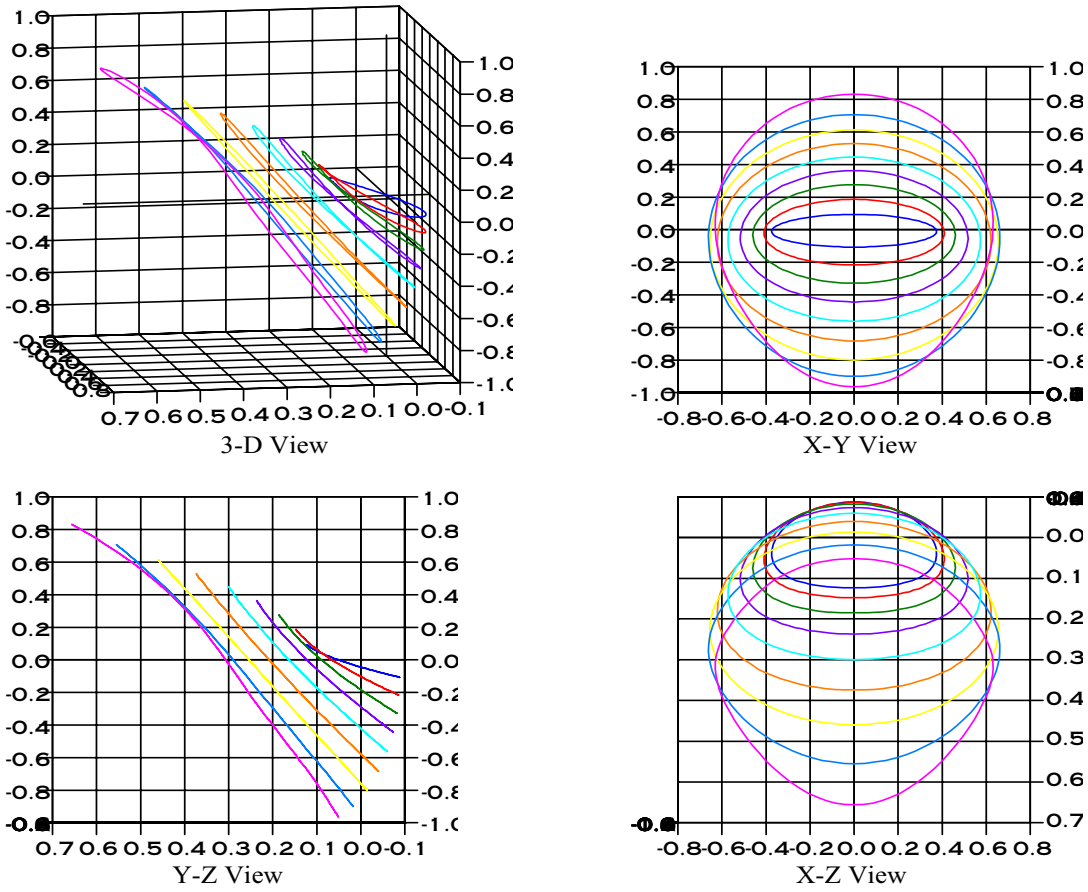

Fig. 1. Halo Orbits in the Earth-Moon System (3-D, X-Y, Y-Z,X-Z).

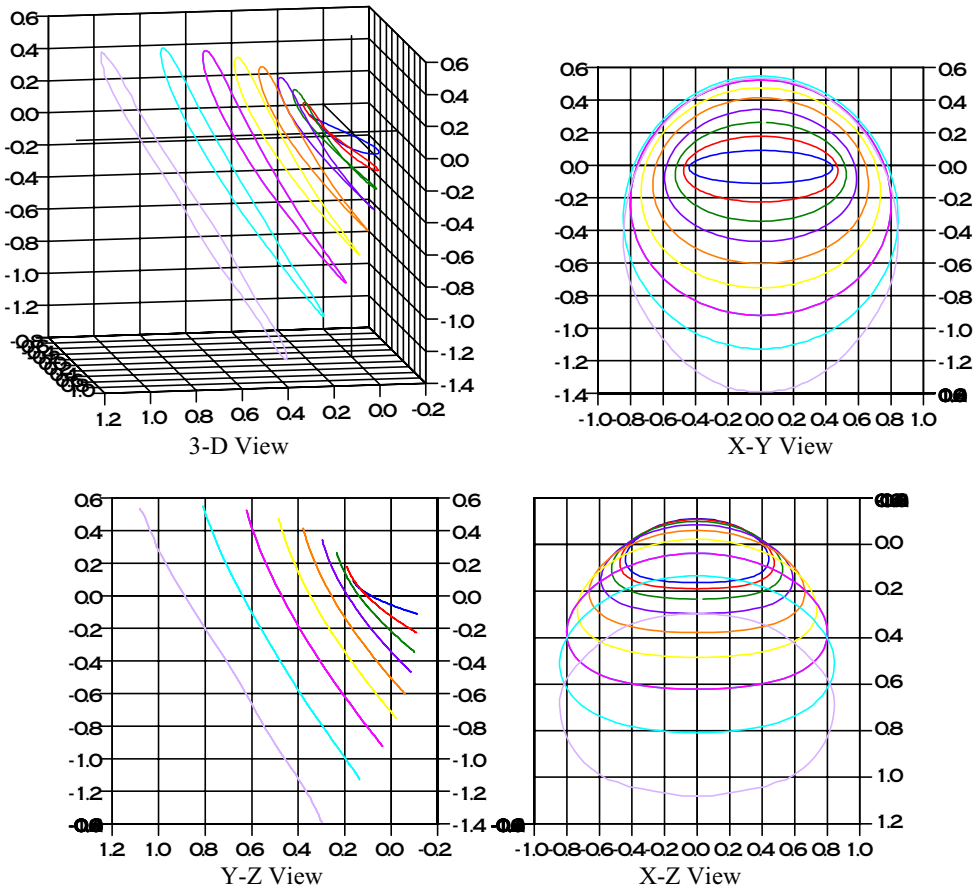

Fig. 2. Examples of Halo Orbits in the Sun-Earth System (3-D, X-Y, Y-Z, X-Z).

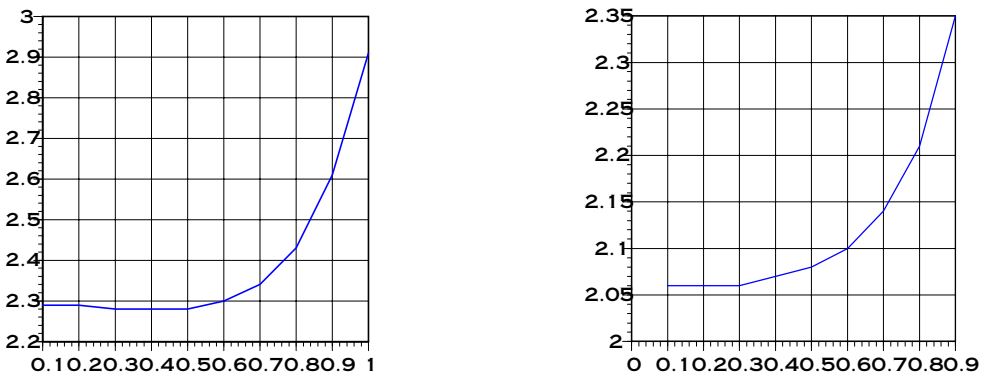

Fig. 3. Frequency of the Halo orbit as a function of β for the Earth-Moon system (left) and Sun-Earth system (right).

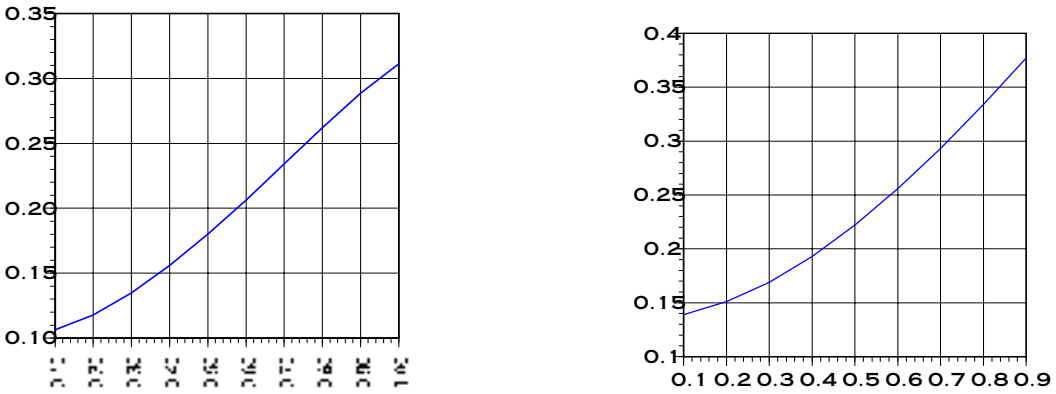

Fig. 4. Amplitude in the x-direction (α) of the Halo orbit as a function of β for the Earth-Moon system (left) and Sun-Earth system (right).

6. Comparison with Numerical Simulations

Having determined a number of solutions with the analytical approach, the next step was to check these results against the exact numerical integration of the restricted three-body problem. The results of this comparison are shown in Figs. 5 and 6 for different values of β for the Sun-Earth system. Initial conditions for the orbits generated by numerical integration were taken equal to those deduced from the analytical estimation. Figure 5 shows the difference between the two orbits, also as function of time. This difference is calculated at every instant of time by

$$\delta = \sqrt{\delta x^2 + \delta y^2 + \delta z^2 + \delta v_x^2 + \delta v_y^2 + \delta v_z^2} \tag{13}$$

Where δx, δy, δz are the differences in the components of the position vector between the trajectory given by the analytical approximation and the trajectory given by the numerical integration and δv_x, δv_y, δv_z are the differences in the components of the velocity vector between the same trajectories. Figure 6 shows both sets of orbits superposed as function of time. Each plot has a collection of orbits generated by the same initial conditions, but integrated over different periods of time. The numbers written at the right of the plots represents the integration time of each trajectory in canonical units (one canonical units is defined such that the period of the orbit is 2π). This procedure was used to determine the time that the orbit is destroyed. Figure 7 shows the orbits individually for the case β = 0.32. It is visible that the destruction of the orbit occurs for a time between 7 and 8.

We can clearly see that the accuracy of the analytical method decreases with larger values of β; this is expected since the size of the non-linear terms is a direct function of the amplitude. Nevertheless, even for moderate-to-large values of the amplitude, the approximation obtained by the Lindsted-Poincaré method is very good.

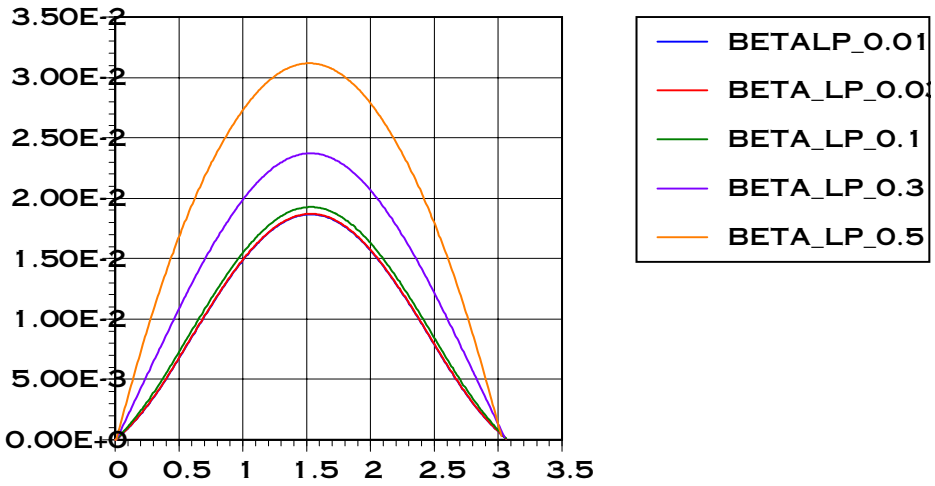

Fig. 5. Difference Between the Two Orbits (Analytical and Numerical) as Function of Time.

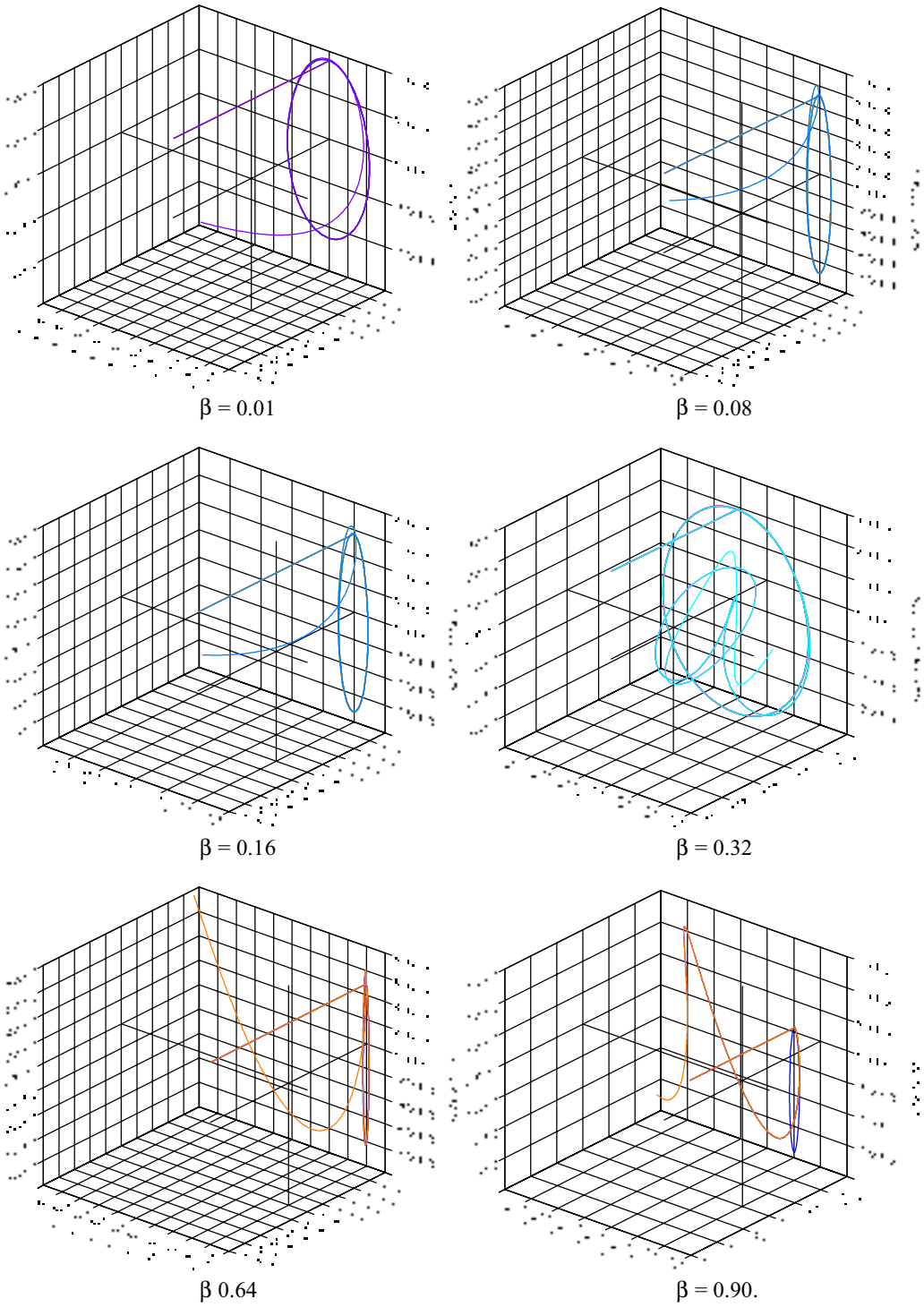

Fig. 6. Analytical and Numerical Trajectories for β = 0.01, 0.08, 0.16, 0.32, 0.64, 0.90.

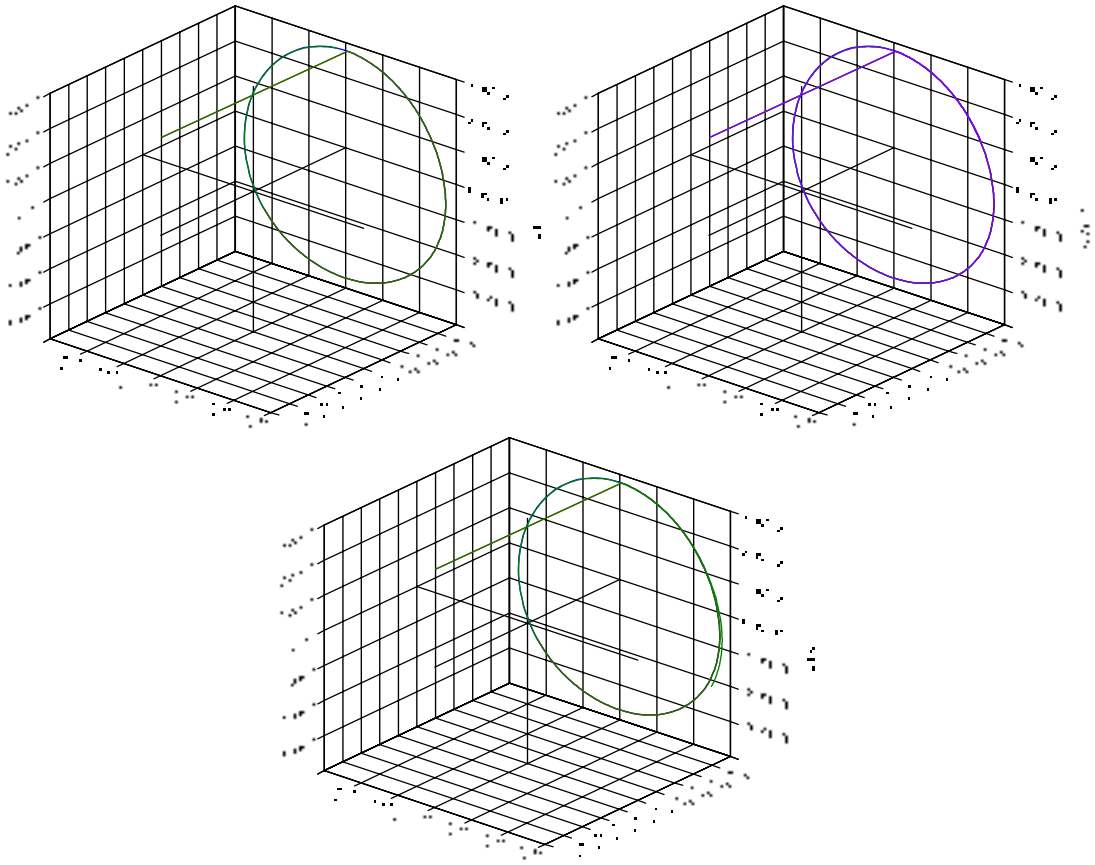

Fig. 7. Time Evolution of the Trajectories for $\beta = 0.32$.

7. Conclusions

In this communication we presented an analytical algorithm to calculate Halo orbits in the circular restricted three-body problem. Several periodic orbits were generated for both the Earth-Moon and the Sun-Earth systems. Comparisons with numerical simulations of the exact equations show that the orbits remain close to each other for about three revolutions, although the exact time is a function of the amplitude. After this interval, the differences between the full and the truncated solution become significant. It is important to bear in mind that these periodic orbits are unstable; thus, any discrepancy between the initial conditions and the center manifold will grow exponentially with time. For this reason, the proximity between the analytical and numerical solutions for as long as three complete revolutions is more than adequate. Another characteristic visible in the results shown in this paper is that in the Sun-Earth system the trajectories are closer to each other than in the Earth-Moon system. This fact occurs because the mass of the Moon (in the Earth-Moon system) relative to the total mass of the system is higher than the mass of the Earth (in the Sun-Earth system) and as a consequence its gravity field acts stronger in the trajectories.

8. Acknowledgments

The authors are grateful to the São Paulo State Science Foundation (FAPESP) for the research grants received under Contracts 2000/14769-4, 2000/7074-0 and 1999/08740-4 and to CNPq (Brazilian National Council for Scientific and Technological Development) for contract 300221/95-9.

9. References

Andreu, M.A. e Simó, C. (1999). Translunar Halo Orbits in the Quasi-Bicircular Problem, em "The Dynamics of Small Bodies in the Solar System", NATO, ASI (Maratea, Italia).

Farquhar, R. W. (1970). The Control and Use of Libration-Point Satellites, NASA TR R-346.

Farquhar, R. W. e Kamel, A.A. (1973). Quasi-Periodic Orbits Around the Translunar Libration Points, *Celestial Mechanics*, **7**, 458.

Gomez, G., Howell, K., Masdemont, J. e Simó, C. (1998). Station-Keeping Strategies for Translunar Libration Point Orbits. *AAS 98-168.*

Gomez, G., Masdemont, J. e Simó, C. (2000). Quasi-Halo Orbits associated with Libration Points, preprint.
Richardson, D.L. (1980). Analytic Costruccion of Periodic Orbits Around the Collinear Points. *Celestial Mechanics*, 22, 241-253.
Szebehely, V. (1967). "Theory of Orbits: The Restricted Problem of Three Bodies", Academic Press, New York.